

Alessandro Granata · Enrico Monzani · Luigi Casella

## Mechanistic insight into the catechol oxidase activity by a biomimetic dinuclear copper complex

Received: 26 March 2004 / Accepted: 23 August 2004 / Published online: 22 September 2004  
© SBIC 2004

**Abstract** The biomimetic catalytic oxidation of 3,5-di-*tert*-butylcatechol by the dicopper(II) complex of the ligand  $\alpha,\alpha'$ -bis{bis[1-(1'-methyl-2'-benzimidazolyl)methyl]amino}-*m*-xylene in the presence of dioxygen has been investigated as a function of temperature and pH in a mixed aqueous/organic solvent. The catalytic cycle occurs in two steps, the first step being faster than the second step. In the first step, one molecule of catechol is oxidized by the dicopper(II) complex, and the copper(II) centers are reduced. From the pH dependence, it is deduced that the active species of the process is the monohydroxo form of the dinuclear complex. In the second step, the second molecule of catechol is oxidized by the dicopper(I)-dioxygen complex formed upon oxygenation of the reduced complex. In both cases, catechol oxidation is an inner-sphere electron transfer process involving binding of the catechol to the active species. The binary catechol-dicopper(II) complex formed in the first step could be characterized at very low temperature ( $-90\text{ }^{\circ}\text{C}$ ), where substrate oxidation is blocked. On the contrary, the ternary complex of dicopper(I)- $\text{O}_2$ -catechol relevant to the second step does not accumulate in solution and could not be characterized, even at low temperature. The investigation of the biphasic kinetics of the catalytic reaction over a range of temperatures allowed the thermodynamic ( $\Delta H^{\circ}$  and  $\Delta S^{\circ}$ ) and activation parameters ( $\Delta H^{\ddagger}$  and  $\Delta S^{\ddagger}$ ) connected with the key steps of the catecholase process to be obtained.

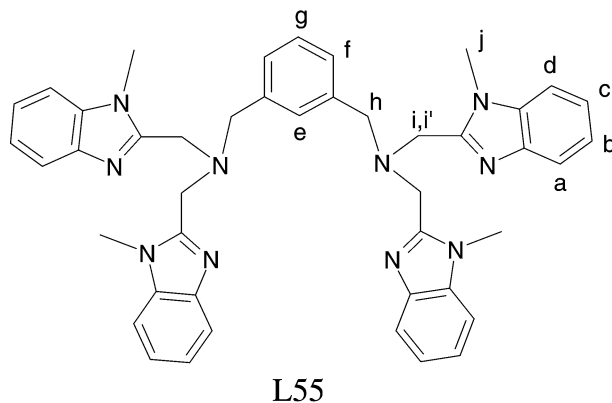
**Keywords** Biomimetic models · Catalysis · Catechols · Copper oxidases · Oxidation

**Abbreviations** DTBCH<sub>2</sub>: 3,5-di-*tert*-butylcatechol · DTBQ: 3,5-di-*tert*-butylquinone · L55:  $\alpha,\alpha'$ -bis{bis[1-(1'-methyl-2'-benzimidazolyl)methyl]amino}-*m*-xylene · LMCT: ligand-to-metal charge transfer

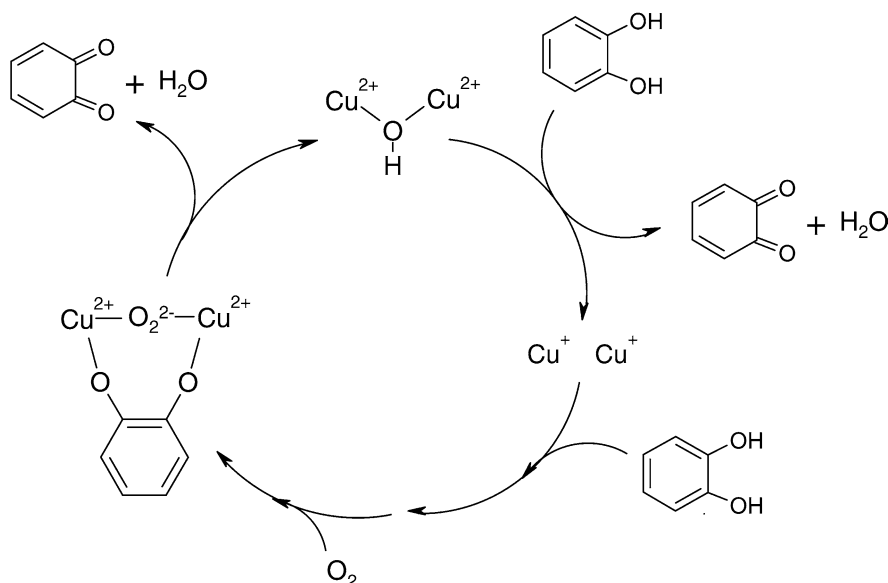
### Introduction

The catalytic oxidation of *ortho*-diphenols to quinones is the only known activity of catechol oxidase [1] and one of the activities of tyrosinase, which is also able to oxidize monophenols to quinones [2]. Dioxygen reduction to water is coupled to the oxidation of two catechol molecules in these processes. Both types of enzyme contain a dinuclear, type 3 Cu center in which each metal ion is coordinated to three histidine ligands. Important details of the mechanism by which catechol oxidase and tyrosinase oxidize catechols are completely unknown. In particular, the mode of substrate binding and product release from the enzyme, and the mode of dioxygen activation and cleavage at the dinuclear copper center, are still under debate [1, 3, 4]. Catecholase activity has been recently associated also with bovine brain Cu-S100B, a small neural protein which binds two Cu ions with type 2 spectroscopic features [5]. However, in this case the ratio between quinone produced and dioxygen consumed is 1:1, and the latter is reduced to hydrogen peroxide. Several model Cu complexes exhibit catecholase activity [6, 7, 8, 9, 10, 11, 12, 13, 14, 15, 16, 17, 18], but thorough mechanistic studies are scarce [11, 12, 13, 14, 15, 16], and in particular only in a few cases has the mode of reduction of dioxygen, to hydrogen peroxide [12, 13, 14] or water [15, 16], been established. The dinuclear copper(II) complex derived from the ligand L55 ( $\alpha,\alpha'$ -bis{bis[1-(1'-methyl-2'-benzimidazolyl)methyl]amino}-*m*-xylene),  $[\text{Cu}_2\text{L55}]^{4+}$ , appears to exhibit the highest activity in the catalytic oxidation of catechols among the available Cu systems [15]. An important feature of the reaction mediated by  $[\text{Cu}_2\text{L55}]^{4+}$  is the possibility to separate the two steps of

A. Granata · E. Monzani · L. Casella (✉)  
Dipartimento di Chimica Generale,  
Università di Pavia, Via Taramelli 12, 27100 Pavia, Italy  
E-mail: bioinorg@unipv.it  
Fax: +39-0382-528544



**Scheme 1** Simplified mechanism of the catechol oxidase catalytic cycle



the catecholase catalytic cycle corresponding to oxidation of the two molecules of catechol (Scheme 1). Herein we report mechanistic details on these two steps, which provide new insight into the catecholase activity of type 3 Cu enzymes.

## Materials and methods

The complexes  $[\text{Cu}_2\text{L55}(\text{H}_2\text{O})_2][\text{ClO}_4]_4$  and  $[\text{Cu}_2\text{L55}(\text{CH}_3\text{CN})_2][\text{ClO}_4]_2$  were prepared as described previously [19]. The catalytic oxidation of 3,5-di-*tert*-butylcatechol (DTBCH<sub>2</sub>) by  $[\text{Cu}_2\text{L55}]^{4+}$  and O<sub>2</sub> was studied at various temperatures in a mixed solvent of 75% methanol/glycerol (7/1 v/v) and 25% (v/v) aqueous 50 mM Hepes buffer at pH 6.8, saturated with atmospheric oxygen. The reactions were followed through the development of the 3,5-di-*tert*-butylquinone (DTBQ) band at 412 nm ( $\epsilon$  1550 M<sup>-1</sup> cm<sup>-1</sup> in the above medium). In each experiment, the curve of quinone absorption versus time was found to be biphasic: a fast initial increase of absorbance, corresponding to the amount of copper catalyst present, was followed by a slower increase due to the catalytic reaction (Fig. 1).

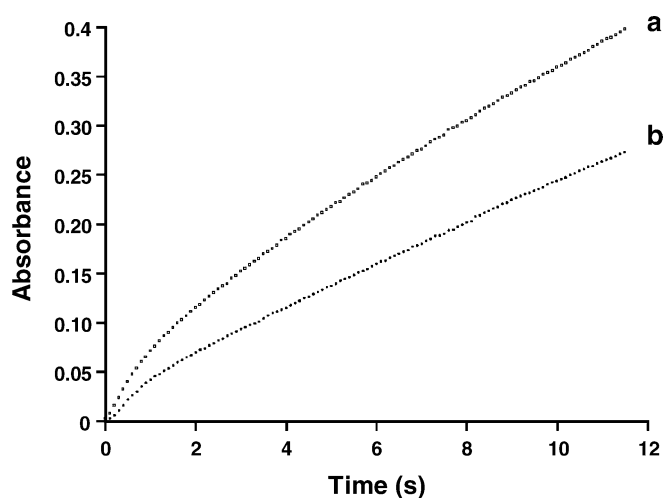


**Fig. 1** Biphasic trace of absorbance versus time curves in typical kinetic experiments of DTBCH<sub>2</sub> oxidation in the mixed solvent of 75% methanol/glycerol (7/1) and 25% (v/v) Hepes buffer (50 mM) at 20 ± 0.1 °C; mixing of the reagents was performed with the stopped-flow apparatus: (a) 0.050 mM  $[\text{Cu}_2(\text{L55})]^{4+}$ ; (b) 0.025 mM  $[\text{Cu}_2(\text{L55})]^{4+}$ ; in both cases,  $[\text{DTBCH}_2]$  was 4 mM

The first step of DTBCH<sub>2</sub> oxidation was studied with an Applied Photophysics model RS-1000 stopped-flow instrument, with 1 ms dead time and 1-cm path-length cell, coupled with a HP 8452A diode array spectrophotometer. The solution of [Cu<sub>2</sub>L55]<sup>4+</sup> (10 μM) in the aqueous/organic solvent was mixed with solutions of variable concentrations of DTBCH<sub>2</sub> (0.2–4 mM) in the same solvent. Upon mixing, the final concentrations of the complex and DTBCH<sub>2</sub> was reduced to one half of the original concentrations. The rate dependence on [DTBCH<sub>2</sub>] was studied in the range from 14 to 33 °C; experiments at lower temperature were hampered by tarnish problems of the cuvette and at higher temperatures the reactions were too fast to give reliable rate data. Temperature was controlled at ±0.1 °C with a thermostat. All the experiments were repeated at least four times. The rates in Δ*A*/s units were calculated from the slope of the trace at 412 nm in the first 2–3 s after mixing of the reagents; the conversion from Δ*A*/s to s<sup>-1</sup> units was made using the quinone extinction coefficient and the complex concentration. The kinetic parameter *k*<sub>1</sub> and the thermodynamic dissociation constant *K*<sub>D1</sub> were obtained by fitting of the rate versus [DTBCH<sub>2</sub>] plots. The above procedure was repeated, changing the pH of the aqueous buffer added to the organic solvent from 6.0 to 8.5. The experiments were performed at constant DTBCH<sub>2</sub> (2 mM) and catalyst (6 μM) concentrations, at 20 ± 0.1 °C. For determining the exact pH of the mixed solvent, the glass electrode was calibrated through the addition of measured quantities of standard perchloric acid solution to a 75% methanol/glycerol (7/1 v/v) and 25% (v/v) water solution, at the desired temperature, according to Gran's method [20]. Blank experiments were carried out in the absence of copper catalyst, but no significant catechol autoxidation was detected in the time range investigated.

The second step of the reaction was studied using a diode array spectrophotometer, in a magnetically stirred and thermostatted (at ±0.1 °C) 1-cm pathlength cell. The rate dependence of [DTBCH<sub>2</sub>] was determined by maintaining the concentration of [Cu<sub>2</sub>L55]<sup>4+</sup> at 2.5 μM and varying the substrate concentration from 0.05 to 5 mM. The temperature dependence of the rate was studied in the 0–27 °C range. All measurements were performed in duplicate. In all cases the reactions showed a biphasic behavior. Since the first step was completed in the mixing time of the solutions, reliable data could be obtained only for the second step, taking the data in the time interval of 5–20 s, where the absorbance variation was linear. At long reaction times, some inactivation of the catalyst was noted. The conversion from Δ*A*/s to s<sup>-1</sup> units was made using the quinone extinction coefficient and the complex concentration, and then dividing the value obtained by 2; the latter operation is required because in each catalytic cycle two quinone molecules are produced (see below). The kinetic parameter *k*<sub>2</sub> and the dissociation constant *K*<sub>D2</sub> were obtained by fitting of the rate versus [DTBCH<sub>2</sub>] plots.

The above procedure was repeated, changing the pH of the aqueous buffer added to the organic solvent from 6.0 to 8.5. The experiments were performed at constant DTBCH<sub>2</sub> (2 mM) and catalyst (6 μM) concentrations, at 20 ± 0.1 °C.

The reaction rates for the two steps of the reaction were also determined with an alternative method. The absorbance at 412 nm versus time profile was fitted to the following equation (see Appendix for details):

$$\text{Abs} = \epsilon_P \times \frac{k_{\text{obs1}} \times [\text{Cu}_2\text{L55}]}{k_{\text{obs1}} + k_{\text{obs2}}} \times \left\{ 2 \times k_{\text{obs1}} \times t - \frac{k_{\text{obs1}} - k_{\text{obs2}}}{k_{\text{obs1}} + k_{\text{obs2}}} \right\} \times [1 - \exp[-(k_{\text{obs1}} + k_{\text{obs2}}) \times t]] \quad (1)$$

where P represents the quinone,  $\epsilon_P$  its molar extinction coefficient at the reading wavelength, and *k*<sub>obs1</sub> and *k*<sub>obs2</sub> the observed kinetic constants for the first and second steps, respectively, so that the rate of each step can be obtained by directly multiplying the observed constant with the [Cu<sub>2</sub>L55]<sup>4+</sup> concentration. This method gave reliable data only using the stopped-flow mixing apparatus.

The experiments at variable O<sub>2</sub> concentration were also performed using the stopped-flow apparatus; the concentrations of DTBCH<sub>2</sub> and [Cu<sub>2</sub>L55]<sup>4+</sup> were maintained fixed at 4 mM and 2.5 μM, respectively, in the cuvette in the usual solvent, at 20 ± 0.1 °C. Solutions of both the substrate and catalyst containing the desired O<sub>2</sub> concentration were prepared by mixing appropriate volumes of a deoxygenated solution and an O<sub>2</sub>-saturated (1 atm) solution of the compounds. Deoxygenation and O<sub>2</sub> saturation of the solutions were performed by bubbling for 20 min pre-equilibrated (with the same solvent) streams of argon or dioxygen, respectively, at constant temperature.

The determination of dissolved dioxygen in the solvent mixture employed for the kinetic measurements was made at different temperatures, three times at each temperature, after equilibration with air, by Winkler's method [21]. The experimental dioxygen concentration ranged from 0.57 mM at 12 °C to 0.50 mM at 27 °C.

The low-temperature experiments were performed using a custom-designed immersible fiber-optic quartz probe (5 mm pathlength, Hellma) fitted to a Schlenk vessel with gas and vacuum inlets and connected to the diode array spectrophotometer. The catechol complex of [Cu<sub>2</sub>L55]<sup>4+</sup> was obtained by adding to an anaerobic solution of the complex (0.2 mM) in degassed methanol at -90 °C a chilled, degassed methanolic solution of DTBCH<sub>2</sub> (1.8 mM final concentration). The solution was kept at low temperature for 3 h, recording spectra from time to time, and then it was slowly warmed to room temperature. A similar experiment was carried out using [Cu<sub>2</sub>L55]<sup>2+</sup> and DTBCH<sub>2</sub>, but no appreciable

spectral changes were detected. The catechol complex of  $[\text{Cu}_2\text{L55}]^{2+}$  could be instead characterized by NMR, by recording anaerobic spectra of the complex in  $\text{CD}_3\text{OD}$  at low temperature in the absence and in the presence of 10 molar equiv DTBCH<sub>2</sub>. The experiments attempting to characterize the ternary complex of  $[\text{Cu}_2\text{L55}]^{2+}$ -O<sub>2</sub>-DTBC were carried out by adding to a degassed methanolic solution of  $[\text{Cu}_2\text{L55}(\text{CH}_3\text{CN})_2]^{2+}$  at  $-90^\circ\text{C}$ , degassed methanolic solutions of DTBCH<sub>2</sub> (to final concentrations up to 3.2 mM), and then adding chilled pure dioxygen (1 atm) to the cold solution and recording optical spectra.

## Results and discussion

The Cu<sup>I</sup> and Cu<sup>II</sup> complexes of the dinucleating ligand L55 constitute one of the few biomimetic systems exhibiting phenol monooxygenase activity [22] and catecholase activity [15]. Both the Cu<sup>I</sup> and Cu<sup>II</sup> complexes have been recently structurally characterized [23]. The previous study of the catalytic oxidation of DTBCH<sub>2</sub> by  $[\text{Cu}_2\text{L55}]^{4+}$  was carried out at pH 5.1 [15]. The mixed solvent of 75% methanol/glycerol (7/1 v/v) and 25% (v/v) aqueous 50 mM Hepes buffer allows good solubility of the reagents, thus extending the investigation of the catecholase reaction over a range of temperatures and pH. Also in this aqueous/organic solvent, the catecholase reaction by  $[\text{Cu}_2\text{L55}]^{4+}$  proceeds with a biphasic rate of DTBQ development (Fig. 1). The initial phase is faster and involves the stoichiometric oxidation of one molecule of catechol per molecule of  $[\text{Cu}_2\text{L55}]^{4+}$ ; this is followed by a second phase which involves the true catalytic process. At longer reaction times, some catalyst degradation occurs; the complex performs at least 70 cycles, at room temperature, before significant inactivation. This process is probably related to the presence of a large amount of water (25% v/v) in the solvent; in fact, when the reaction was performed in a 30/1 (v/v) methanol/buffer solution, no significant degradation was observed, even at longer reaction times [15].

We used two different methods for the analysis of the data. In the first one the two steps were analyzed separately; the initial rate was used to obtain the observed rate constant for the stoichiometric process, while the turnover rate in the catalytic phase was used for the second step. In the second method, the rate constants were obtained by fitting the development of the quinone absorbance with time to Eq. 1. In spite of the differences in the two methods of analysis, the results obtained were identical.

The observed rate constants for both the reaction steps were found to exhibit hyperbolic dependence on DTBCH<sub>2</sub> concentration (Fig. 2). In addition, the rate of the first step was unaffected by changing the dioxygen concentration of the reaction solution (data not shown). In contrast, the rate of the second step depends linearly on  $[\text{O}_2]$  (Fig. 3), independent of the catechol concen-

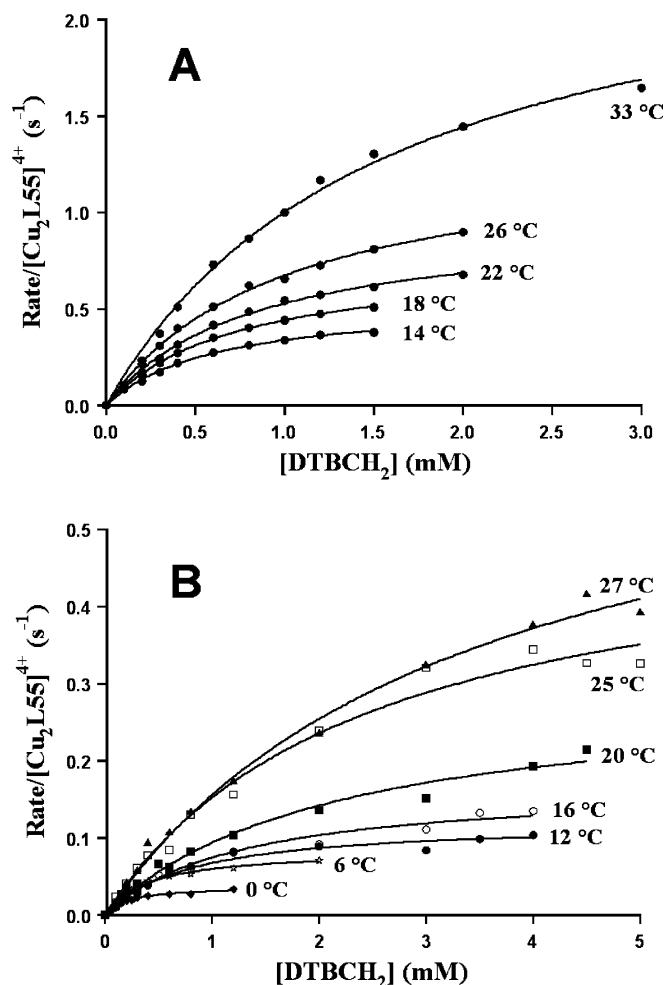
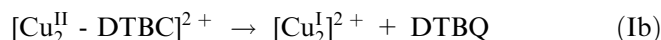
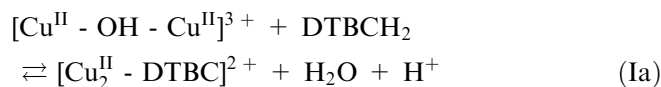


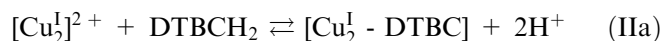
**Fig. 2A, B** Rate dependence of the oxidation of DTBCH<sub>2</sub> catalyzed by  $[\text{Cu}_2\text{L55}]^{4+}$  on catechol concentration in the mixed solvent of 75% methanol/glycerol (7/1) and 25% (v/v) Hepes buffer (50 mM, pH 6.8) at different temperatures. **A** First phase: mixing of the reagents was performed with the stopped-flow apparatus; 5  $\mu\text{M}$   $[\text{Cu}_2\text{L55}]^{4+}$ ; fitting of the curve was performed with Eq. 2. **B** Second phase: 2.5  $\mu\text{M}$   $[\text{Cu}_2\text{L55}]^{4+}$ ; fitting of the curve was performed with Eq. 3

tration. The nonzero value for the rate in the absence of dioxygen observed in the plot of Fig. 3 is probably due to unavoidable leaks in the transfer of the deoxygenated and partially oxygenated solutions. These results can be rationalized on the basis of the following mechanism:

### 1. First Step:



### 2. Second step:



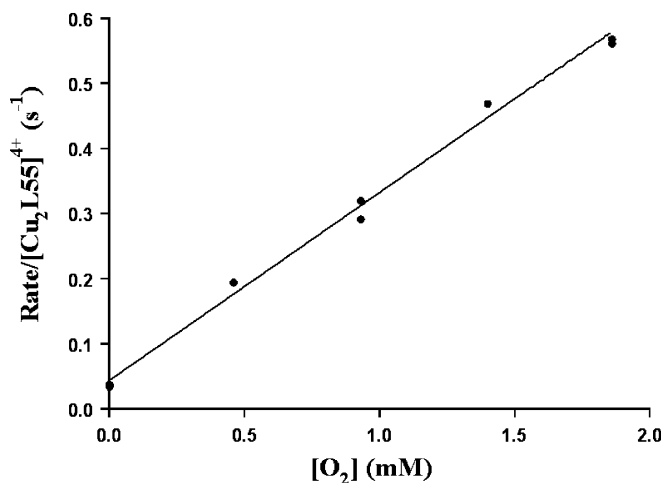
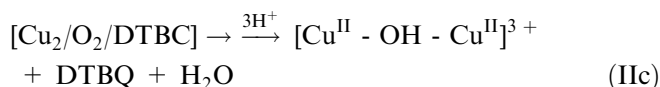
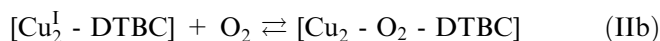


Fig. 3 Rate dependence for the second step of the oxidation of DTBCH<sub>2</sub> (4 mM) catalyzed by [CuL55]<sup>4+</sup> (2.5 μM) on dioxygen concentration in the mixed solvent of 75% methanol/glycerol (7/1) and 25% (v/v) Hepes buffer (50 mM) at pH 6.8 at 20 ± 0.1 °C



The first phase of the reaction is connected to reactions Ia and Ib and consists of binding catechol to the [Cu<sub>2</sub>L55]<sup>4+</sup> complex, followed by electron transfer to give the quinone. The rate is given by the equation (see Appendix):

$$\text{rate} = \frac{k_1 \times [\text{DTBCH}_2] \times [\text{complex}]}{K_{\text{D1}} + [\text{DTBCH}_2]} \quad (2)$$

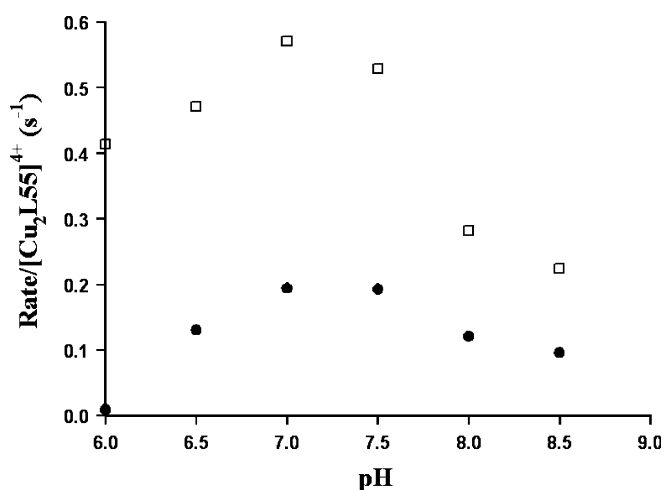
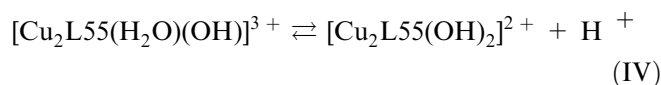
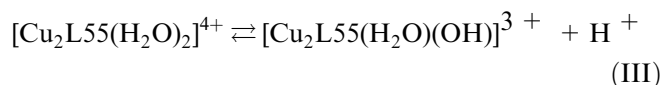


Fig. 4 Rate dependence for the first (*open squares*) and second (*solid circles*) steps of the oxidation of DTBCH<sub>2</sub> (2 mM) catalyzed by [Cu<sub>2</sub>L55]<sup>4+</sup> (6 μM) on the pH in the mixed solvent of 75% methanol/glycerol (7/1) and 25% (v/v) Hepes buffer (50 mM) at 20 ± 0.1 °C

where  $K_{\text{D1}}$  represents the dissociation constant for the [Cu<sub>2</sub><sup>II</sup>/DTBC] adduct, i.e. reverse of reaction Ia, and  $k_1$  the rate constant for reaction Ib.

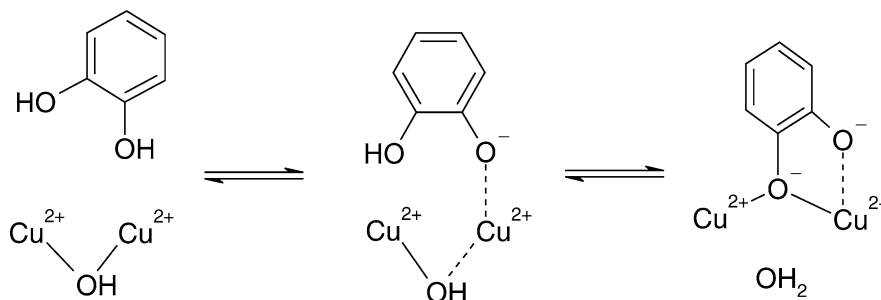
In reaction Ia, the active form of the [Cu<sub>2</sub>L55]<sup>4+</sup> catalyst is represented as a monohydroxo species. In fact, the [Cu<sub>2</sub>L55]<sup>4+</sup> complex undergoes pH-dependent dissociation equilibria from a moderately coupled bis(aqua)-dicopper(II) form to a strongly magnetically coupled bis( $\mu$ -hydroxo)-dicopper(II) form [23]:



with the intermediate monohydroxo species appreciably present between pH 6 and 8, but in lower than 20% abundance. The  $pK_a$  values for dissociation of bound water in reactions III and IV were determined previously as 6.93 and 6.25, respectively (in acetonitrile/water, 4/1 v/v) [23]. The bis( $\mu$ -dimethoxo)-dicopper(II) complex derived from [Cu<sub>2</sub>L55(OH)<sub>2</sub>]<sup>2+</sup> by water-methanol interchange has been characterized by X-ray crystallography [23]. When the rate of the first step of the catecholase reaction was studied as a function of the pH of the medium, it was found that the rate was maximal around pH 7, but it dropped dramatically above pH ≈ 7.5 (Fig. 4). Taking into account that deprotonation of DTBCH<sub>2</sub> is favored at higher pH, the rate profile parallels the distribution curve of the monohydroxo species [Cu<sub>2</sub>L55(H<sub>2</sub>O)(OH)]<sup>3+</sup> [23], while the bis( $\mu$ -hydroxo) species [Cu<sub>2</sub>L55(OH)<sub>2</sub>]<sup>2+</sup>, which is dominant above pH ≈ 6.5, is catalytically inactive. This is probably due to the difficulty of the catechol to attack the tightly bridged Cu<sub>2</sub>(OH)<sub>2</sub> core. For the same reason, an analogous monohydroxo-dicopper(II) intermediate was found to be critical for hydrogen peroxide binding and activation in the biomimetic dicopper(II) complex with the closely related ligand L66 [24]. It is interesting to note that a monohydroxo-bridged dicopper(II) center is also contained in the structure of oxidized catechol oxidase [25] and is assumed to be present in met-tyrosinase [26]. The bridging hydroxo group may be essential to remove the second proton of the catechol residue and favor the binding of the substrate in a bridging mode (Scheme 2).

To characterize the catechol-[Cu<sub>2</sub>L55]<sup>4+</sup> interaction in the first step, a methanolic solution of [Cu<sub>2</sub>L55]<sup>4+</sup> was reacted anaerobically with excess DTBCH<sub>2</sub> at -90 °C. The dominant UV/Vis ligand-to-metal charge transfer (LMCT) features of the fraction of bis( $\mu$ -hydroxo) species [19] present in solution ( $\lambda_{\text{max}}$  320 and 350 nm) were slowly replaced by weaker absorptions at 345 and 440 nm, attributable to LMCT bands of the catecholate complex (Fig. 5). The resulting spectrum is quite similar to that of the complex formed by [Cu<sub>2</sub>L55]<sup>4+</sup> with the dianion of methyl 3,4-di-

**Scheme 2** The catechol binding process to the dicopper(II) center



hydroxybenzoate that, due to the electron-withdrawing substituent on the catechol ring, is stable and could be isolated and characterized previously [22]. In the present case, warming the solution of the  $[\text{Cu}^{\text{II}}_2\text{-DTBC}]$  complex to room temperature results in quantitative catechol oxidation and  $\text{Cu}^{\text{II}}$  reduction. The multicomponent structure of the LMCT band suggests that catecholate binds as a bridging ligand to the dicopper(II) complex, as this is a common feature observed in the LMCT spectra of dicopper(II) complexes containing other bridging ligands like azide [19, 27] or even peroxide [28, 29]. As a matter of fact, chelated catecholate mononuclear  $\text{Cu}^{\text{II}}$  complexes exhibit a single LMCT band [18, 23]. The  $\eta^2:\eta^1$  bridging mode proposed for catecholate binding in Scheme 2 is based on the results of a recent spectroscopic investigation of nitrocatecholate-copper(II) complexes [30].

The second phase of the reaction involves the global turnover, reactions Ia–Ic, where the rate-determining step is reaction Iic. Catechol binding to the  $\text{Cu}^{\text{I}}_2$  species in reaction Ia occurs as a pre-equilibrium before dioxygen binding, and accounts for the observed substrate

saturation behavior. This pre-equilibrium is required because  $[\text{Cu}_2\text{L55}]^{2+}$  does not form a stable dioxygen complex even at low temperature, due to the poor coordination of the ligand L55 tertiary amino groups to the  $\text{Cu}^{\text{I}}$  ions, as shown by the crystal structure of the complex [23]. Charge donation from bound catechol to the  $\text{Cu}^{\text{I}}$  centers partially compensates this effect, facilitating the formation of the dioxygen adduct. We have tried to characterize the binding of catechol to  $[\text{Cu}_2\text{L55}(\text{CH}_3\text{CN})_2]^{2+}$  by spectroscopic methods in anaerobic conditions. Catecholate complex formation does not bear useful near-UV features but can be followed by NMR (Fig. 6). Since at the concentrations required for the NMR experiment the presence of base causes precipitation of the complex in the presence of the catechol, an excess of free  $\text{DTBCH}_2$  had to be used to force the binding process. To reduce the effect of exchange phenomena, due to the kinetic lability of  $\text{Cu}(\text{I})$ , the spectra were recorded at low temperature. The proton signals of the benzimidazole, xylyl, and methylene groups of the ligand are slightly shifted and both the bound  $\text{CH}_3\text{CN}$  molecules of the starting complex are clearly displaced upon formation of the catechol- $[\text{Cu}_2\text{L55}]^{2+}$  complex. Since the signals of the L55 residues bound to both  $\text{Cu}^{\text{I}}$  atoms are affected and the spectrum of the  $\text{Cu}^{\text{I}}_2$ -catechol complex maintains the symmetric pattern present in that of the starting  $[\text{Cu}_2\text{L55}(\text{CH}_3\text{CN})_2]^{2+}$  complex, catechol appears to bind to both  $\text{Cu}^{\text{I}}$  atoms. Although we cannot discriminate the mode of binding of the catechol, we believe that in order to keep the two  $\text{Cu}^{\text{I}}$  ions in close proximity to favor the dioxygen binding step (reaction Iib), DTBC must act as a symmetric, likely  $\eta^1:\eta^1$  bridging, ligand in this case (Scheme 3).

Attempts to characterize the ternary complex of  $[\text{Cu}_2\text{L55}]^{2+}\text{-O}_2\text{-DTBC}$  by UV/Vis or NMR techniques at low temperature were unsuccessful, even in the presence of large excess  $\text{DTBCH}_2$ . Thus, the ternary complex does not accumulate in solution during turnover. The observed data could be explained considering a slow oxygenation of the complex  $[\text{Cu}^{\text{I}}_2\text{-DTBC}]$ , reaction Iib, followed by faster catechol oxidation. This hypothesis agrees with the kinetic behavior but can be discarded on the basis of the analysis of the activation parameters of the reaction (see below). A second possibility to explain the lack of accumulation of the ternary complex

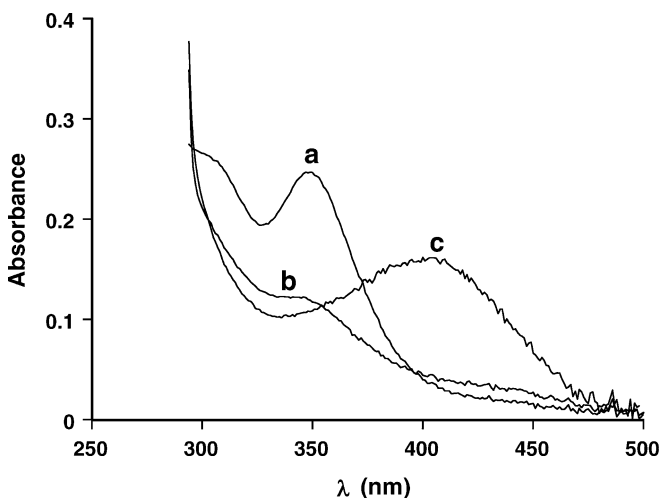
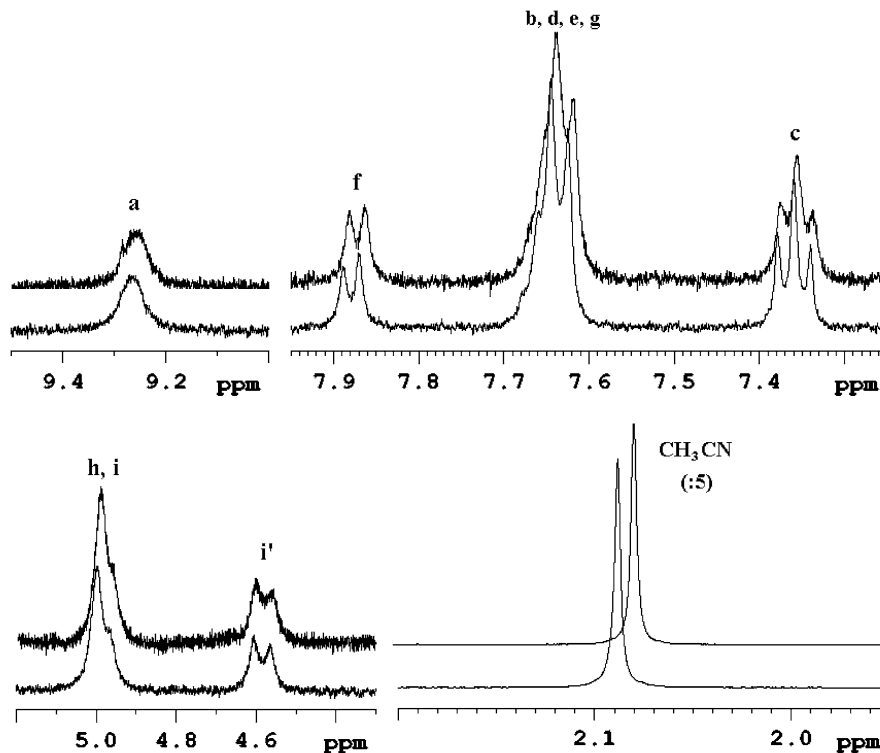


**Fig. 5** Electronic spectra recorded anaerobically in methanol solution at  $-90^\circ\text{C}$  of: (a)  $[\text{Cu}_2(\text{L55})]^{4+}$  (0.2 mM) and (b) its complex with  $\text{DTBCH}_2$  (1.8 mM). Spectrum (c) shows the stoichiometric formation of DTBQ after warming the solution to room temperature. When the solution was exposed to air, quantitative conversion of  $\text{DTBCH}_2$  into DTBQ occurred

**Fig. 6** NMR spectra of  $[\text{Cu}_2\text{L55}(\text{CH}_3\text{CN})_2]^{2+}$  (lower trace) and the complex in the presence of 10 molar equiv DTBCH<sub>2</sub> (upper trace) in CD<sub>3</sub>OD at -40 °C under anaerobic conditions. Labeling refers to the structure of L55. Signals due to excess DTBCH<sub>2</sub> are not shown. The chemical shift of methyl protons j at 3.77 ppm for  $[\text{Cu}_2\text{L55}]^{2+}$  is little affected by DTBC binding. The spectra are basically unchanged, but decrease in resolution at still lower temperature



in the second step considers that oxygenation is faster than electron transfer, but that the equilibrium IIb is shifted to the left, so that only a minor fraction of the complex is present in solution as a ternary complex. This implies that quinone formation according to reaction IIc is preceded by two successive equilibria, that is coordination of DTBCH<sub>2</sub> (reaction IIa) and then O<sub>2</sub> (reaction IIb) to  $[\text{Cu}_2\text{L55}]^{2+}$ . The rate of the process then becomes (see Appendix):

$$\text{rate} = \frac{k_{\text{IIc}} \times K_{\text{O}_2} \times [\text{O}_2] \times [\text{DTBCH}_2] \times [\text{complex}]}{K_{\text{D}_2} + [\text{DTBCH}_2] + K_{\text{O}_2} \times [\text{O}_2] \times [\text{DTBCH}_2]} \approx \frac{k_2 \times [\text{DTBCH}_2] \times [\text{complex}]}{K_{\text{D}_2} + [\text{DTBCH}_2]} \quad (3)$$

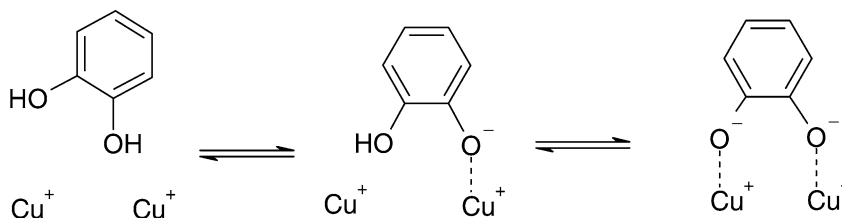
where  $k_{\text{IIc}}$  represents the rate constant for reaction IIc,  $K_{\text{O}_2}$  the dioxygen affinity constant in the ternary complex, and  $k_2 = k_{\text{IIc}} \times K_{\text{O}_2} \times [\text{O}_2]$ . Equation 3 agrees with the observation that the rate of the second step depends both on substrate and dioxygen concentrations.

When the rate of the second step was analyzed as a function of the pH of the medium (Fig. 4), it was found

that the maximum activity occurs above pH 7. The reaction rates drops dramatically at acidic pH. Probably this is due to protonation of the ligand, with concomitant release of copper(I), or protonation of the ternary complex of  $[\text{Cu}_2\text{L55}]^{2+}$ -O<sub>2</sub>-DTBC, with concomitant release of hydrogen peroxide; the last option is consistent with the observed catalyst degradation at long reaction times.

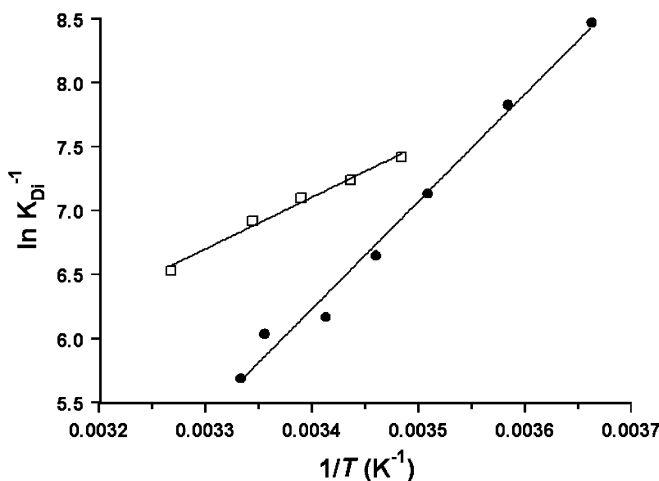
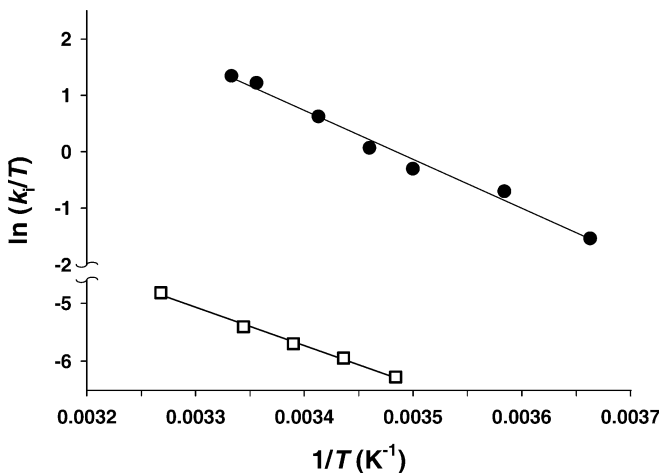
Fitting the rate data obtained at different temperatures with Eq. 2 for the first step, and Eq. 3 for the second step, allowed the determination of  $k_1$ ,  $K_{\text{D}_1}$ ,  $k_2$  and  $K_{\text{D}_2}$  (data at 20 °C in Table 1). According to the proposed mechanism,  $K_{\text{D}_1}$  and  $K_{\text{D}_2}$  refer to the catechol dissociation constant for the Cu<sup>II</sup><sub>2</sub> and Cu<sup>I</sup><sub>2</sub> forms of the complex, respectively. The temperature dependence of  $K_{\text{D}_1}^{-1}$  and  $K_{\text{D}_2}^{-1}$ , through the van't Hoff equation (Fig. 7), gives the  $\Delta H^\circ$  and  $\Delta S^\circ$  values for reactions Ia and IIa, respectively (Table 1). Surprisingly,  $\Delta H^\circ$  is less favorable for the first step, involving Cu<sup>II</sup><sub>2</sub>, with respect to the second step, involving Cu<sup>I</sup><sub>2</sub>. This is due to the fact that, in the first step, binding of the catechol to  $[\text{Cu}_2\text{L55}(\text{H}_2\text{O})(\text{OH})]^{3+}$

**Scheme 3** The catechol binding process to the dicopper(I) center



**Table 1** Kinetic and thermodynamic parameters for the two steps of the catalytic catecholase reaction

	Step 1	Step 2
$k_i$ (s <sup>-1</sup> ) <sup>a</sup>	0.87 ± 0.03 (20 °C)	0.29 ± 0.02 (20 °C)
$K_{D_i}$ (mM) <sup>a</sup>	0.77 ± 0.06 (20 °C)	2.1 ± 0.3 (20 °C)
$\Delta H^\ddagger$ (kJ mol <sup>-1</sup> )	55 ± 2	72 ± 3
$\Delta S^\ddagger$ (J mol <sup>-1</sup> K <sup>-1</sup> )	-59 ± 7	54 ± 11
$\Delta H^\circ$ (kJ mol <sup>-1</sup> )	-34 ± 2	-70 ± 3
$\Delta S^\circ$ (J mol <sup>-1</sup> K <sup>-1</sup> )	-55 ± 7	-185 ± 12

<sup>a</sup> $i=1, 2$ **Fig. 7** van't Hoff plots for the two steps of the catalytic oxidation of DTBCH<sub>2</sub> by [Cu<sub>2</sub>L55]<sup>4+</sup> in a mixed solvent of 75% methanol/glycerol (7/1) and 25% Hepes buffer (50 mM) at pH 6.8: open squares, first step ( $K_{D_i}^{-1}=K_{D_1}^{-1}$ ); solid circles, second step ( $K_{D_i}^{-1}=K_{D_2}^{-1}$ )**Fig. 8** Eyring plots for the two steps of the catalytic oxidation of DTBCH<sub>2</sub> by [Cu<sub>2</sub>L55]<sup>4+</sup> in a mixed solvent of 75% methanol/glycerol (7/1) and 25% Hepes buffer (50 mM) at pH 6.8: solid circles, first step ( $k_i=k_1$ ); open squares, second step ( $k_i=k_2/[O_2]$ )

occurs with displacement of the hydroxo group (reaction Ia). On the other hand, this OH group keeps the Cu<sup>II</sup> centers of the dinuclear complex in close

proximity and this favors, from an entropy point of view ( $\Delta S^\circ$  is less negative), the coordination of DTBCH<sub>2</sub> as a bridge between the two metal ions. The large negative  $\Delta S^\circ$  term in the case of [Cu<sub>2</sub>L55]<sup>2+</sup> is probably related to the fact that the two ligand arms binding the Cu<sup>I</sup> centers are largely free to move and catechol binding to both metal ions strongly reduces the mobility of the molecule. Overall, the binding is stronger in the first step than in the second step ( $K_{D_1}^{-1} > K_{D_2}^{-1}$ ), due to the less unfavorable entropy term.

The activation parameters for reactions Ib, IIb and IIc were obtained through the temperature dependence of  $k_1$  and  $k_2$ , respectively (Fig. 8, Table 1). For step 1,  $k_1$  measures the rate of electron transfer of reaction Ib, which is followed by a presumably fast quinone release. The  $\Delta H^\ddagger$  value is moderately large, its magnitude being determined by the difference in redox potential of the two partners and by the overlap between the orbitals involved. Interestingly,  $\Delta S^\ddagger$  has a negative value, in spite that reaction Ib occurs with an increase in the number of species.

For the analysis of the rate of the second step, we note that  $k_2$  is the combination of an electron transfer rate constant, a binding constant and [O<sub>2</sub>] ( $k_2 = k_{IIc} \times K_{O_2} \times [O_2]$ ). Therefore, for the determination of the  $\Delta H^\ddagger$  and  $\Delta S^\ddagger$  parameters for the second step it was necessary to determine the value of [O<sub>2</sub>] at each temperature and apply the Eyring equation to  $k_2/[O_2]$  (Fig. 8). Since  $k_2/[O_2] = k_{IIc} \times K_{O_2}$ , the observed activation parameters are combinations of kinetic and thermodynamic parameters:

$$\Delta H^\ddagger = \Delta H_{ET}^\ddagger + \Delta H^\circ_{\text{oxygen}} \quad (4)$$

$$\Delta S^\ddagger = \Delta S_{ET}^\ddagger + \Delta S^\circ_{\text{oxygen}} \quad (5)$$

where  $\Delta H_{ET}^\ddagger$  and  $\Delta S_{ET}^\ddagger$  refer to the electron transfer process from bound catechol to the Cu<sub>2</sub>O<sub>2</sub> core in reaction IIc, and  $\Delta H^\circ_{\text{oxygen}}$  and  $\Delta S^\circ_{\text{oxygen}}$  refer to the oxygenation equilibrium of reaction IIb. The range of  $\Delta H^\circ_{\text{oxygen}}$  values for a variety of dinuclear Cu<sup>I</sup> complexes related to [Cu<sub>2</sub>L55]<sup>2+</sup> extends from -28 to -74 kJ mol<sup>-1</sup> [31]. We expect that, in the present case,  $\Delta H^\circ_{\text{oxygen}}$  will be less favorable, i.e. shifted toward the positive range, as [Cu<sub>2</sub>L55]<sup>2+</sup> does not form a stable dioxygen complex. In any case, the  $\Delta H^\ddagger$  value for the second step of the catalytic cycle is larger than that for the first step, making reactions IIb and IIc the rate-determining steps for the catechol oxidation. The large  $\Delta H^\ddagger$  for reaction IIc is probably essentially determined by the cleavage of the O-O bond in the transition state, in agreement with theoretical calculations [4]. In addition, as opposed to the first step,  $\Delta S^\ddagger$  is now large and positive, in spite of the fact that  $\Delta S^\circ_{\text{oxygen}}$  is expected to be large and negative, with values ranging from -100 to -250 J K<sup>-1</sup> mol<sup>-1</sup> [31]. For reaction IIb,  $\Delta S^\circ_{\text{oxygen}}$  probably approaches the more negative end of this range, due to sizeable steric



crowding in the ternary complex of  $[\text{Cu}_2\text{L55}]^{2+}\text{-O}_2\text{-DTBC}$ . As a consequence,  $\Delta S^\ddagger_{\text{ET}} = \Delta S^\ddagger - \Delta S^\circ_{\text{oxyg}}$  must have a large positive value, probably because passing from the ternary complex to the transition state the partial cleavage of the O–O and Cu–O(catechol) bonds relieves the steric crowding.

As stated above, the lack of accumulation of the ternary complex in the second step could in principle be explained also by a slow oxygenation of the complex  $[\text{Cu}^{\text{I}}_2\text{-DTBC}]$  (reaction IIb), followed by faster catechol oxidation. The rate equation describing this process would be analogous to Eq. 3, with  $k_2 = k_{\text{ox-yg}} \times [\text{O}_2]$  (see Appendix), and in that case  $\Delta S^\ddagger$  would refer to the oxygenation process of reaction IIb. However, the observation of a positive  $\Delta S^\ddagger$  contrasts this possibility, since it would imply a negative activation entropy. In fact, oxygenation studies performed on dinuclear  $\text{Cu}^{\text{I}}$  complexes systematically show large negative values of  $\Delta S^\ddagger$ , ranging from  $-66$  to  $-167 \text{ J K}^{-1} \text{ mol}^{-1}$  [31].

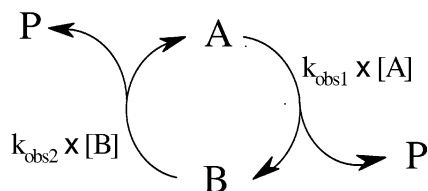
In summary, the present investigation analyzes the catalytic catechol oxidase activity by the biomimetic dinuclear copper complex derived from the ligand L55. The elementary steps of the catalytic cycle have been separated, allowing, for the first time, the determination of the kinetic and thermodynamic parameters controlling the two phases of the process. The data obtained on this model system can be useful for the interpretation of the intimate mechanisms of the catecholase reactions promoted by type 3 copper enzymes such as catechol oxidase and tyrosinase, which are still completely unclear.

**Acknowledgements** This work was supported by the Italian MIUR (PRIN project) and by the University of Pavia. The CIRCMSB is gratefully acknowledged for a fellowship to A.G.

## Appendix

### Derivation of the equations

Scheme 4 shows a catalytic cycle containing two consecutive irreversible reactions that depend on the first order on the catalyst concentration. The mechanism can be described by the following equations system, which neglects the changes in the rate due to the consumption of substrate (S), i.e. considering [S] and  $[\text{O}_2]$  approximately constant. A and B are two forms of the catalyst and P is the product:



Scheme 4

$$\frac{d[\text{P}]}{dt} = k_{\text{obs1}} \times [\text{A}] + k_{\text{obs2}} \times [\text{B}] \quad (\text{A1})$$

$$\frac{d[\text{A}]}{dt} = k_{\text{obs2}} \times [\text{B}] - k_{\text{obs1}} \times [\text{A}] \quad (\text{A2})$$

$$\frac{d[\text{B}]}{dt} = k_{\text{obs1}} \times [\text{A}] - k_{\text{obs2}} \times [\text{B}] \quad (\text{A3})$$

Considering that the catalyst is present in solution initially in the A form:

$$[\text{A}_0] = [\text{A}] + [\text{B}] \quad (\text{A4})$$

From Eqs. A2 and A4, considering that  $[\text{A}] = [\text{A}_0]$  at  $t = 0$ , the dependence of the concentration of the two catalyst forms versus time can be obtained:

$$[\text{A}] = \frac{[\text{A}_0]}{k_{\text{obs1}} + k_{\text{obs2}}} \times \{k_{\text{obs2}} + k_{\text{obs1}} \times \exp[-(k_{\text{obs1}} + k_{\text{obs2}}) \times t]\} \quad (\text{A5})$$

$$[\text{B}] = [\text{A}_0] \times \left\{ 1 - \frac{1}{k_{\text{obs1}} + k_{\text{obs2}}} \times [k_{\text{obs2}} + k_{\text{obs1}} \times \exp[-(k_{\text{obs1}} + k_{\text{obs2}}) \times t]] \right\} \quad (\text{A6})$$

The rate equation can be obtained introducing [A] and [B] into Eq. A1:

$$\frac{d[\text{P}]}{dt} = \frac{k_{\text{obs1}} \times [\text{A}_0]}{k_{\text{obs1}} + k_{\text{obs2}}} \times \{2 \times k_{\text{obs2}} + (k_{\text{obs1}} - k_{\text{obs2}}) \times \exp[-(k_{\text{obs1}} - k_{\text{obs2}}) \times t]\} \quad (\text{A7})$$

The rate constants  $k_{\text{obs1}}$  and  $k_{\text{obs2}}$  can be obtained measuring the reaction rates at  $t \rightarrow 0$  (initial phase of the reaction) and at  $t \rightarrow \infty$  (turnover):

$$t \rightarrow 0: \quad \frac{d[\text{P}]}{dt} = k_{\text{obs1}} \times [\text{A}_0] \quad (\text{A8})$$

$$t \rightarrow \infty: \quad \frac{d[\text{P}]}{dt} = \frac{2 \times k_{\text{obs1}} \times k_{\text{obs2}} \times [\text{A}_0]}{k_{\text{obs1}} + k_{\text{obs2}}} \quad (\text{A9})$$

From the reaction rate in the first stage of the reaction,  $k_{\text{obs1}}$  can be obtained from Eq. A8. From the reaction rate during turnover,  $k_{\text{obs1}}$  and Eq. A9,  $k_{\text{obs2}}$  can be obtained.

An alternative way for the determination of the rate constants is based on the monitoring of the accumulation of the product with time. Solving the differential Eq. A7 and considering that, at  $t = 0$ ,  $[\text{P}] = 0$ , we obtain:

$$[\text{P}] = \frac{k_{\text{obs1}} \times [\text{A}_0]}{k_{\text{obs1}} + k_{\text{obs2}}} \times \left\{ 2 \times k_{\text{obs1}} \times t - \frac{k_{\text{obs1}} - k_{\text{obs2}}}{k_{\text{obs1}} + k_{\text{obs2}}} \times [1 - \exp[-(k_{\text{obs1}} + k_{\text{obs2}}) \times t]] \right\} \quad (\text{A10})$$

Fitting the [P] data as a function of time with Eq. A10 gives directly the two rate constants.

The same equations apply also in more complicated mechanisms where the two steps are composite reactions but with a linear dependence of the rate versus [A] and [B] if the variation of the other reagents can be neglected (i.e. if they are in excess or only the initial part of the reaction is considered). In such cases, the catalytic constants are an ensemble of different parameters. In particular, this is the case described in the present paper where the composite reactions are reactions Ia and Ib for the first step and reactions IIa to IIc for the second step.

### 1. First step:

The reaction of the species A requires an initial fast binding of the substrate followed by the formation of the product and the B form of the catalyst:



This is a simple first-order reaction preceded by a pre-equilibrium; its rate law is:

$$\text{rate} = \frac{k_1 \times [S] \times [A]}{K_{D1} + [S]} = k_{\text{obs1}} \times [A] \quad (A13)$$

It is important to note that  $k_{\text{obs1}}$  depends on the substrate concentration with a Michaelis–Menten-type behavior.

### 2. Second step:

The reaction of species B requires the initial binding of the substrate followed by the binding of a second molecule (O) and thus by the product formation and the restoration of species A:



The rate equation depends on the relative rates of the processes. Here we consider two different cases; in both of them the substrate binding is assumed a fast step.

(a) The rate constant for the reaction with O is larger than that of product formation:  $k_{O1} \times [O]$  and  $k_{O-1} > k_p$ . The second step represents two pre-equilibrium binding processes followed by a slow reaction. The corresponding rate law is:

$$\text{rate} = \frac{k_p \times K_O \times [O] \times [S] \times [B]}{K_{D2} + [S] + K_O \times [O] \times [S]} = k_{\text{obs2}} \times [B] \quad (A17)$$

If  $K_O$  ( $K_O = k_{O1}/k_{O-1}$ ) has a small value, the equilibrium A15 is shifted to the left and the equation is reduced to:

$$\begin{aligned} \text{rate} &= \frac{k_p \times K_O \times [O] \times [S] \times [B]}{K_{D2} + [S] + K_O \times [O] \times [S]} \\ &\approx \frac{k_p \times K_O \times [O] \times [S] \times [B]}{K_{D2} + [S]} = k_{\text{obs2}} \times [B] \end{aligned} \quad (A18)$$

where:

$$k_{\text{obs2}} = \frac{k_p \times K_O \times [O] \times [S]}{K_{D2} + [S]} \quad (A19)$$

(b) The reaction of BS with O is the rate-determining step, while reaction A16 is a fast process:  $k_{O1} \times [O] < k_p$ . Reaction A16 does not contribute to the rate. The mechanism can be simply view as a pre-equilibrium A14 followed by the irreversible slow reaction A15:

$$\text{rate} = \frac{k_{O1} \times [O] \times [S] \times [B]}{K_{D2} + [S]} = k_{\text{obs2}} \times [B] \quad (A20)$$

For both the cases (a) and (b),  $k_{\text{obs2}}$  depends linearly on [O] and depends on [S] with Michaelis–Menten-type behavior.

## References

- Gerdeman C, Eicken C, Krebs B (2002) *Acc Chem Res* 35:183–191
- Solomon EI, Sundaram UM, Machonkin TE (1996) *Chem Rev* 96:2563–2605
- Decker H, Dillinger R, Tucek F (2000) *Angew Chem Int Ed* 39:1591–1595
- Siegbahn PEM (2003) *J Biol Inorg Chem* 8:567–576
- Senior S, Mans LL, Van Guilder HD, Kelly KA, Hendrich MP, Elgren TE (2003) *Biochemistry* 42:4392–4397
- Oishi N, Nishida Y, Ida K, Kida S (1980) *Bull Chem Soc Jpn* 53:2847–2850
- Malachowski MR, Huynh HB, Tomlinson LJ, Kelly RS, Furbee JW Jr (1995) *J Chem Soc Dalton Trans* 31–36
- Than R, Feldman AA, Krebs B (1999) *Coord Chem Rev* 182:211–241
- Torelli S, Belle C, Gautier-Luneau I, Pierre JL, Saint-Aman E, Latour JM, Le Pape L, Luneau D (2000) *Inorg Chem* 39:3526–3536
- Belle C, Beguin C, Gautier-Luneau I, Hamman S, Philouze C, Pierre JL, Thomas F, Torelli S, Saint-Aman E, Bonin M (2002) *Inorg Chem* 41:479–491
- Speier G (1986) *J Mol Catal* 37:259–267
- Chyn JP, Urbach FL (1991) *Inorg Chim Acta* 189:157–163
- Balla J, Kiss T, Jameson RF (1992) *Inorg Chem* 31:58–62
- Selmezi K, Réglie M, Giorgi M, Speier G (2003) *Coord Chem Rev* 245:191–201
- Monzani E, Quinti L, Perotti A, Casella L, Gullotti M, Randaccio L, Geremia S, Nardin G, Faleschini P, Tabbi G (1998) *Inorg Chem* 37:553–562
- Monzani E, Battaini G, Perotti A, Casella L, Gullotti M, Santagostini L, Nardin G, Randaccio L, Geremia S, Zanello P, Opromolla G (1999) *Inorg Chem* 38:5359–5369
- Santagostini L, Gullotti M, Monzani E, Casella L, Dillinger R, Tucek F (2000) *Chem Eur J* 6:519–522
- Battaini G, Monzani E, Casella L, Santagostini L, Pagliarin R (2000) *J Biol Inorg Chem* 5:262–268
- Casella L, Carugo O, Gullotti M, Garofani S, Zanello P (1993) *Inorg Chem* 32:2056–2067

20. Rossotti FJC, Rossotti HJ (1965) *Chem Educ* 42:375–378
21. Clesceri LS, Greenberg AE, Eaton AD (1998) *Standard methods for the examination of water and wastewater*, 20th edn. American Public Health Association, Washington, DC
22. Casella L, Monzani E, Gullotti M, Cavagnino D, Cerina G, Santagostini L, Ugo R (1996) *Inorg Chem* 35:7516–7525
23. Battaini G, Casella L, Gullotti M, Monzani E, Nardin G, Perotti A, Randaccio L, Santagostini L, Heinemann FW, Schindler S (2003) *Eur J Inorg Chem* 1197–1205
24. Battaini G, Monzani E, Perotti A, Para C, Casella L, Santagostini L, Gullotti M, Dillinger R, Näther C, Tuzcek F (2003) *J Am Chem Soc* 125:4185–4198
25. Klabunde T, Eicken C, Sacchetti JC, Krebs B (1998) *Nat Struct Biol* 5:1084–1090
26. Land EJ, Ramsden CA, Riley PA (2003) *Acc Chem Res* 36:300–308
27. Pate JE, Ross PK, Thamann TJ, Reed CA, Karlin KD, Sorrell TN, Solomon EI (1989) *J Am Chem Soc* 111:5198–5209
28. Solomon EI, Tuzcek F, Root DE, Brown CA (1994) *Chem Rev* 94:827–856
29. Mirica LM, Ottenwaelder X, Stack TDP (2004) *Chem Rev* 104:1013–1045
30. Plenge T, Dillinger R, Santagostini L, Casella L, Tuzcek F (2004) *Z Anorg Allg Chem* 629:2258–2265
31. Karlin KD, Zuberbühler AD (1999) In: Reedijk J, Bouwman E (eds) *Bioinorganic catalysis*. Dekker, New York, pp 469–534